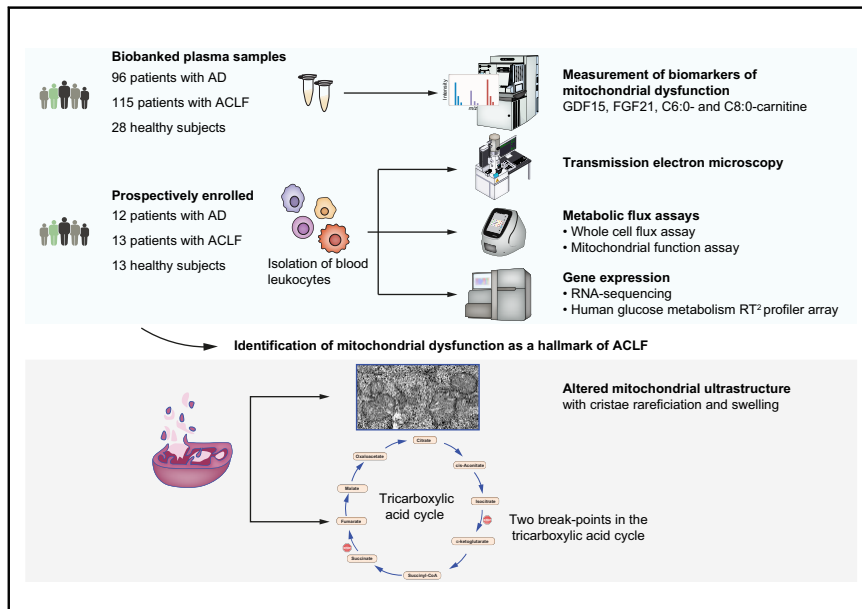


Mitochondrial dysfunction governs immunometabolism in leukocytes of patients with acute-on-chronic liver failure

Graphical abstract



Authors

Ingrid W. Zhang, Anna Curto, Cristina López-Vicario, ..., Javier Fernández, Vicente Arroyo, Joan Clària

Correspondence

jclaria@clinic.cat (J. Clària).

Lay summary

Patients at advanced stages of liver disease have dismal prognosis due to vital organ failures and the lack of treatment options. In this study, we report that the functioning of mitochondria, which are known as the cell powerhouse, is severely impaired in leukocytes of these patients, probably as a consequence of intense inflammation. Mitochondrial dysfunction is therefore a hallmark of advanced liver disease.

Highlights

- Metabolic and transcriptional phenotypes of leukocytes from patients with ACLF were assessed.
- Two break-points were discovered in the tricarboxylic cycle of leukocytes in ACLF.
- Biomarkers of mitochondrial dysfunction correlated with inflammation and gene sets related to leukocyte activation.
- Leukocyte mitochondrial dysfunction is a hallmark of ACLF.



Mitochondrial dysfunction governs immunometabolism in leukocytes of patients with acute-on-chronic liver failure

Ingrid W. Zhang^{1,2}, Anna Curto², Cristina López-Vicario^{1,2}, Mireia Casulleras^{1,2},
Marta Duran-Güell^{1,2}, Roger Flores-Costa^{1,2}, Benoît Colsch³, Ferran Aguilar²,
Ana M. Aransay^{4,5}, Juan José Lozano⁵, María Hernández-Tejero⁶, David Toapanta⁶,
Javier Fernández^{2,5,6}, Vicente Arroyo², Joan Clària^{1,2,5,7,*}

¹Biochemistry and Molecular Genetics Service, Hospital Clínic-IDIBAPS, Barcelona, Spain; ²European Foundation for the Study of Chronic Liver Failure (EF Clif) and Grifols Chair, Barcelona, Spain; ³Laboratoire d'Etude du Métabolisme des Médicaments, CEA, INRA, Université Paris Saclay, MetaboHUB, F-91191 Gif-sur-Yvette, France; ⁴CIC bioGUNE, Parque Tecnológico de Bizkaia, Derio, Bizkaia, Spain; ⁵CIBERehd, Barcelona, Spain; ⁶Liver ICU, Liver Unit, Hospital Clínic-IDIBAPS, Barcelona, Spain; ⁷Department of Biomedical Sciences, University of Barcelona, Barcelona, Spain

Background & Aims: Patients with acute-on-chronic liver failure (ACLF) present a systemic hyperinflammatory response associated with increased circulating levels of small-molecule metabolites. To investigate whether these alterations reflect inadequate cell energy output, we assessed mitochondrial morphology and central metabolic pathways with emphasis on the tricarboxylic acid (TCA) cycle in peripheral leukocytes from patients with acutely decompensated (AD) cirrhosis, with and without ACLF.

Methods: The study included samples from patients with AD cirrhosis (108 without and 128 with ACLF) and 41 healthy individuals. Leukocyte mitochondrial ultrastructure was visualized by transmission electron microscopy and cytosolic and mitochondrial metabolic fluxes were determined by assessing NADH/FADH₂ production from various substrates. Plasma GDF15 and FGF21 were determined by Luminex and acylcarnitines by LC-MS/MS. Gene expression was analyzed by RNA-sequencing and PCR-based glucose metabolism profiler array.

Results: Mitochondrial ultrastructure in patients with advanced cirrhosis was distinguished by cristae rarefaction and swelling. The number of mitochondria per leukocyte was higher in patients, accompanied by a reduction in their size. Increased FGF21 and C6:0- and C8:0-carnitine predicted mortality whereas GDF15 strongly correlated with a gene set signature related to leukocyte activation. Metabolic flux analyses revealed increased energy production in mononuclear leukocytes from patients with preferential involvement of extra-mitochondrial pathways, supported by upregulated expression of genes encoding enzymes of the glycolytic and pentose phosphate pathways. In patients with ACLF, mitochondrial function analysis uncovered break-points in the TCA cycle at the isocitrate dehydrogenase and succinate dehydrogenase level, which were bridged by

anaplerotic reactions involving glutaminolysis and nucleoside metabolism.

Conclusions: Our findings provide evidence at the cellular, organelle and biochemical levels that severe mitochondrial dysfunction governs immunometabolism in leukocytes from patients with AD cirrhosis and ACLF.

Lay summary: Patients at advanced stages of liver disease have dismal prognosis due to vital organ failures and the lack of treatment options. In this study, we report that the functioning of mitochondria, which are known as the cell powerhouse, is severely impaired in leukocytes of these patients, probably as a consequence of intense inflammation. Mitochondrial dysfunction is therefore a hallmark of advanced liver disease.

© 2021 The Authors. Published by Elsevier B.V. on behalf of European Association for the Study of the Liver. This is an open access article under the CC BY-NC-ND license (<http://creativecommons.org/licenses/by-nc-nd/4.0/>).

Introduction

Acute-on-chronic liver failure (ACLF) is a syndrome which develops in patients with acutely decompensated (AD) cirrhosis and is characterized by different combinations of organ failures resulting in high short-term mortality.^{1,2} Accumulating evidence has highlighted that ACLF is associated with intense systemic inflammation and severe immune paralysis.^{3,4} During acute inflammation, immune cells rewire their cellular metabolism to meet the high energy demand, linking metabolic processes to the regulation of immune cell responses, a phenomenon that has been termed immunometabolism.⁵ In this context, mitochondria – as the organelles in which intracellular biochemical pathways converge – are the cell energy powerhouses and their dysfunction is implicated in a variety of diseases such as neurodegenerative disorders, sepsis and heart failure.

Mitochondrial dysfunction is a constant feature in many chronic liver diseases.⁶ Untargeted metabolomics recently uncovered profoundly altered metabolic pathways in patients with AD cirrhosis and ACLF, including evidence that dysfunctional mitochondria might participate in disease development.⁷ In this investigation performed within the frame of the prospective

Keywords: acute decompensated cirrhosis; ACLF; immune cells; metabolic phenotype; mitochondria; RNA-seq.

Received 22 December 2020; received in revised form 4 August 2021; accepted 4 August 2021; available online 25 August 2021

* Corresponding author. Address: Hospital Clínic, EF Clif, Travessera de Gràcia 11, 08021 Barcelona Spain, Tel.: +34 932 271 400.

E-mail address: jclaria@clinic.cat (J. Clària).

<https://doi.org/10.1016/j.jhep.2021.08.009>



European-wide CANONIC study including 1,343 hospitalized patients with AD cirrhosis, elevated serum levels of hexanoyl (C6:0)- and octanoyl (C8:0)-carnitine, which are markers of incomplete mitochondrial fatty acid β -oxidation, were described in patients with ACLF.⁷ In addition, features of increased levels of metabolites of the glucuronate pathway and intermediates of the pentose phosphate pathway (PPP) were observed.⁷ Furthermore, patients with ACLF displayed higher abundance of proteinogenic and ketogenic amino acids (AAs) and their derivatives in the blood.^{7,8}

In view of these findings, we hypothesized that mitochondria-based pathways are less efficiently used in patients with ACLF and that altered energy production dictates immune cell responses and immunometabolism in these patients. This hypothesis was tested in peripheral blood leukocytes considering 3 premises. First, mitochondrial dysfunction in leukocytes is associated with exaggerated systemic inflammation and oxidative stress.^{9,10} Second, inflammation is energetically expensive¹¹ and requires a trade-off of nutrients and energy between immune cells and organ function homeostasis, which may lead to peripheral organ hypometabolism and organ failures. And third, mitochondrial alterations in circulating leukocytes have been correlated with mitochondrial dysfunction in peripheral tissues and organs such as the heart.¹² We assessed our hypothesis using two approaches. The first was of a descriptive nature, comprising the examination of mitochondrial ultrastructure by transmission electron microscopy (TEM) and evaluation of established biomarkers of mitochondrial dysfunction. The second approach was mechanistic and aimed at the analysis of metabolic and transcriptomic phenotypes of circulating leukocytes from patients with AD cirrhosis and ACLF.

Patients and methods

Patients

The study used biobanked plasma and serum samples from 96 patients with AD cirrhosis without ACLF (a group hereafter called “AD”) and 115 patients with AD cirrhosis with ACLF (a group hereafter called “ACLF”) from the CANONIC study, along with 28 healthy individuals (HIs). For TEM, metabolic fluxes and gene expression analyses, peripheral blood mononuclear cells (PBMCs) and polymorphonuclear leukocytes (PMNs) were isolated from patients with AD and ACLF (n = 25) and HIs (n = 13) recruited at the Liver Intensive Care Unit and the Hospital Clínic of Barcelona Blood Bank, respectively. The baseline clinical and laboratory data are shown in [Tables S1-2](#). Complete information is given in the [supplementary patients and methods](#).

Cell isolation and assessment of whole cell flux analysis and mitochondrial function assays

PBMCs and PMNs were isolated by Ficoll-Hypaque. Whole cell flux analysis and mitochondrial function assays were performed using PM-M1 and MitoPlate S-1 assays, respectively. Independent plates were used for each individual and samples were not pooled. Both assays are based on the production of NADH and FADH₂ from various substrates/intermediates, which feed electrons to the electron transport chain (ETC) (see [supplementary patients and methods](#) and [Tables S3-4](#) for detailed lists of substrates/intermediates).

TEM

PBMCs were examined under JEOL J1010 TEM (Akishima, Japan), and the morphometric analysis was performed as described in the [supplementary patients and methods](#).

Gene expression

Gene expression was assessed by Human Glucose Metabolism RT² profiler array (Qiagen), RNA-sequencing (RNA-seq) and real-time PCR (see [supplementary patients and methods](#)).

Detection of biomarkers of mitochondrial dysfunction and inflammation

Plasma levels of fibroblast growth factor (FGF) 21, growth differentiation factor (GDF) 15 and 13 cytokines/chemokines were measured by Luminex technology (see [supplementary patients and methods](#)). Serum levels of acylcarnitines and other laboratory parameters were acquired from the existing CANONIC databases.⁷

Data analysis

Results are presented as mean \pm SEM or median with interquartile range (IQR) as appropriate. For single comparisons, Student's unpaired *t* test for parametric and Mann-Whitney test for nonparametric distribution were used. For multiple comparisons, Kruskal-Wallis test was used for nonparametric distribution, followed by Dunn's post hoc testing. Spearman (Spearman's rho, rs) was applied for not normally distributed variables correlations. For more detailed information see [supplementary patients and methods](#).

Results

Altered mitochondrial ultrastructure of circulating leukocytes in patients with AD and ACLF

TEM images taken at different magnifications of leukocytes from HIs and patients are shown in [Fig. 1A](#). Abnormally shaped mitochondria with cristae rarefaction were seen in PBMCs from patients with AD, compared to the normal conformation seen in HIs. PBMCs from patients with AD displayed autophagic vacuoles with signs of mitophagy, *i.e.* cytoplasmic inclusions engulfed by double-membranes containing mitochondria ([Fig. 1A](#), red arrow). Mitochondria from patients with ACLF showed more apparent cristae rarefaction, swelling and lack of connection than those from patients with AD ([Fig. 1A](#)). These alterations peaked in ACLF-3, wherein mitochondrial ultrastructure was severely disorganized, suggesting extensive degradation of these organelles ([Fig. 1A](#)). These findings indicate that leukocytes from patients with AD and ACLF display typical features of primary mitochondrial disorders.¹³ Of interest, the number of mitochondria per cell was significantly higher in patients with AD and ACLF than in HIs ([Fig. 1B](#)), whereas the length/width ratio, area and perimeter of each mitochondrion were smaller in patients than in HIs ([Fig. 1C](#)). The number of mitochondria and their area were not associated with survival ([Fig. S1A](#)) and did not correlate with the MELD (model for end-stage liver disease) or the CLIF-C OF (Chronic Liver Failure Consortium organ failure) scores ([Fig. S1B](#)). Consistent with previous reports,^{14,15} these alterations were not seen in liver tissue from patients with AD, in whom mitochondria were of average appearance albeit with frequent electron-dense granules in the mitochondrial matrix ([Fig. S1C](#)).

Elevated circulating biomarkers of mitochondrial dysfunction in patients with AD and ACLF

GDF15 and FGF21 are mitokines induced by mitochondrial dysfunction in an activating transcription factor 4 (ATF4)-dependent manner and are regarded as circulating markers for inherited mitochondrial disorders.^{16,17} As shown in Fig. 2A-B, plasma GDF15 and FGF21 levels increased in a staggered fashion from HIs to patients with AD and then to those with ACLF. GDF15 was able to discern ACLF-1 from AD (Fig. 2A), whereas FGF21 was able to distinguish between AD and ACLF-3 as well as between ACLF-2 and ACLF-3 (Fig. 2B). We also calculated the acylcarnitine to free carnitine ratio, an indicator of mitochondrial fatty acid β -oxidation.¹⁸ Patients with ACLF exhibited an increased acylcarnitine/free carnitine ratio in comparison to HIs and those with AD (Fig. 2C), which was mainly attributed to increased short-chain acylcarnitines (Fig. S2A). Medium-chain C6:0- and C8:0-carnitine, which are part of the blood metabolite fingerprint discriminating ACLF from AD,⁷ showed the highest significant correlation with FGF21 (Fig. S2B). In contrast, long-chain C16:0- and C18:2-carnitine negatively correlated with mitokines (Fig. S2B), probably reflecting the first peroxisomal passage in the metabolism of long-chain fatty acids.¹⁹ The predictive value of these biomarkers was assessed by conducting a multivariate risk analysis, which revealed that FGF21, C6:0- and C8:0-carnitine predict mortality in ACLF taking into account the competing risk of liver transplantation (Fig. 2D). Higher levels of these biomarkers were observed at study inclusion in patients with ACLF who did not survive during the 28-day follow-up (Fig. S2C). C6:0- and C8:0-carnitine also predicted outcome in AD (Fig. 2D). Moreover, they positively correlated with classical markers of inflammation (*i.e.* C-reactive protein and white blood cell count) (Fig. S2D). Levels of C6:0-carnitine were higher in patients with bacterial infection (Fig. S3A) whereas FGF21 levels were lower in patients with HCV-etiology in comparison to alcohol-associated cirrhosis (Fig. S3B). Stratification according to the type of organ failures revealed higher levels of biomarkers of mitochondrial dysfunction in patients with kidney failure (Fig. S4).

Relationship between mitochondrial dysfunction and leukocyte activation at the cytokinome and transcriptome level

To determine whether mitochondrial dysfunction is associated with activation/functionality of circulating leukocytes, we correlated plasma levels of GDF15 and FGF21 with those of cytokines/chemokines in 5 HIs and 13 prospectively recruited patients with AD (of whom 8 had ACLF). GDF15 showed a strong positive correlation with macrophage inflammatory protein-1 α and - β and a moderate correlation with interleukin (IL)-1 β , whereas FGF21 positively correlated with monocyte chemoattractant protein-1, IL-1 α and IL-6 (Fig. 2E). We also collected PBMCs from these patients to perform RNA-seq. Gene set enrichment analysis of the most significantly regulated gene sets showed that most of the upregulated pathways were predominantly related to the activation of immune cells (*i.e.* granule formation, phagocytosis, cytokine production/secretion and antigen processing) in both AD and ACLF (Fig. 2F). Importantly, the ATP synthesis-coupled electron transport gene set was significantly upregulated in AD but not in ACLF, probably reflecting mitochondrial failure (Fig. 2F). This ATP synthesis-related gene set was the most representative amid a cluster of 5 gene sets

related to mitochondrial function, including respiration and ETC (Fig. S5A). We also calculated the correlation between GDF15 and FGF21 and the normalized enrichment score of each of the top 50 upregulated gene sets and identified positive correlations between these biomarkers and activation of immune cells (Fig. 2G). For instance, GDF15 strongly correlated with cytokine and chemokine production and macrophage activation and FGF21 correlated with antigen processing. We further browsed the RNA-seq database for ATF4, the hepatic expression of which has been associated with mitochondrial dysfunction in patients with alcohol-related liver disease.²⁰ As shown in Fig. S5B, no changes in ATF4 expression were seen in peripheral leukocytes from patients with AD and ACLF in comparison to HIs. Moreover, we did not detect changes in hepatic ATF4 expression in patients with AD, except in 1 patient who presented with liver failure (Fig. S5C).

PBMCs from patients with AD and ACLF undergo rewiring of cellular metabolism: boosting extra-mitochondrial pathways

We next wondered whether mitochondrial dysfunction in patients with AD and ACLF was accompanied by changes in leukocyte metabolism. To explore this, we performed whole cell flux analysis in PBMCs using PM-M1 plates and observed that D-glucose was the most preferred substrate, although PBMCs from AD and ACLF used a wider range of carbon and nitrogen sources to generate energy than HIs (Fig. 3A). In absolute amounts, PBMCs from AD and ACLF generated more energy than those from HIs (Fig. 3A, Fig. S6-7), probably to satisfy the high-energy demand of activated leukocytes. PBMCs from ACLF showed a higher utilization of sugars and sugar derivatives than those from AD (Fig. S8), although the overall energy output was similar (Fig. S9A). The increased energy turnover was also evident when the substrates were grouped according to the different categories of macro- and micro-molecules (Fig. 3B). The higher utilization of substrates was further illustrated in a supervised clustergram of the row-wise scaled values of the different substrates according to their biochemical family (Fig. 3C). Calculation of the relative amount of energy produced from substrates strictly metabolized in mitochondria with respect to the total energy produced by the cell revealed that PBMCs from AD and ACLF utilized extra-mitochondrial pathways for much more of their energy production (Fig. 3D). This is consistent with the reduced blood lactate/pyruvate ratio, a surrogate marker of the cytosolic NADH/NAD⁺ ratio (Fig. 3E, Fig. S9B), suggesting an increased glycolytic flux in detriment to mitochondrial TCA cycle activity.²¹

To obtain deeper insight into the TCA cycle, we performed metabolic flux analysis using MitoPlate S-1, hereafter referred to as mitochondrial function assays. Succinate was the most favored mitochondrial substrate in PBMCs from HIs and AD, whereas this position was ceded to malate in ACLF (Fig. 4A). Sn-Glycerol 3-phosphate (G3P), which participates in energy generation through the G3P shuttle, was the second most preferred substrate in AD (Fig. 4A). Fig. 4B shows the unsupervised hierarchical cluster analysis of the row-wise scaled values of the different substrates metabolized through mitochondrial pathways, in which G3P together with L-leucine and its derivative α -ketoisocaproic acid were utilized more in patients with AD than in HIs and those with ACLF. Fig. 4B also shows that PBMCs from patients with ACLF preferentially utilized TCA cycle

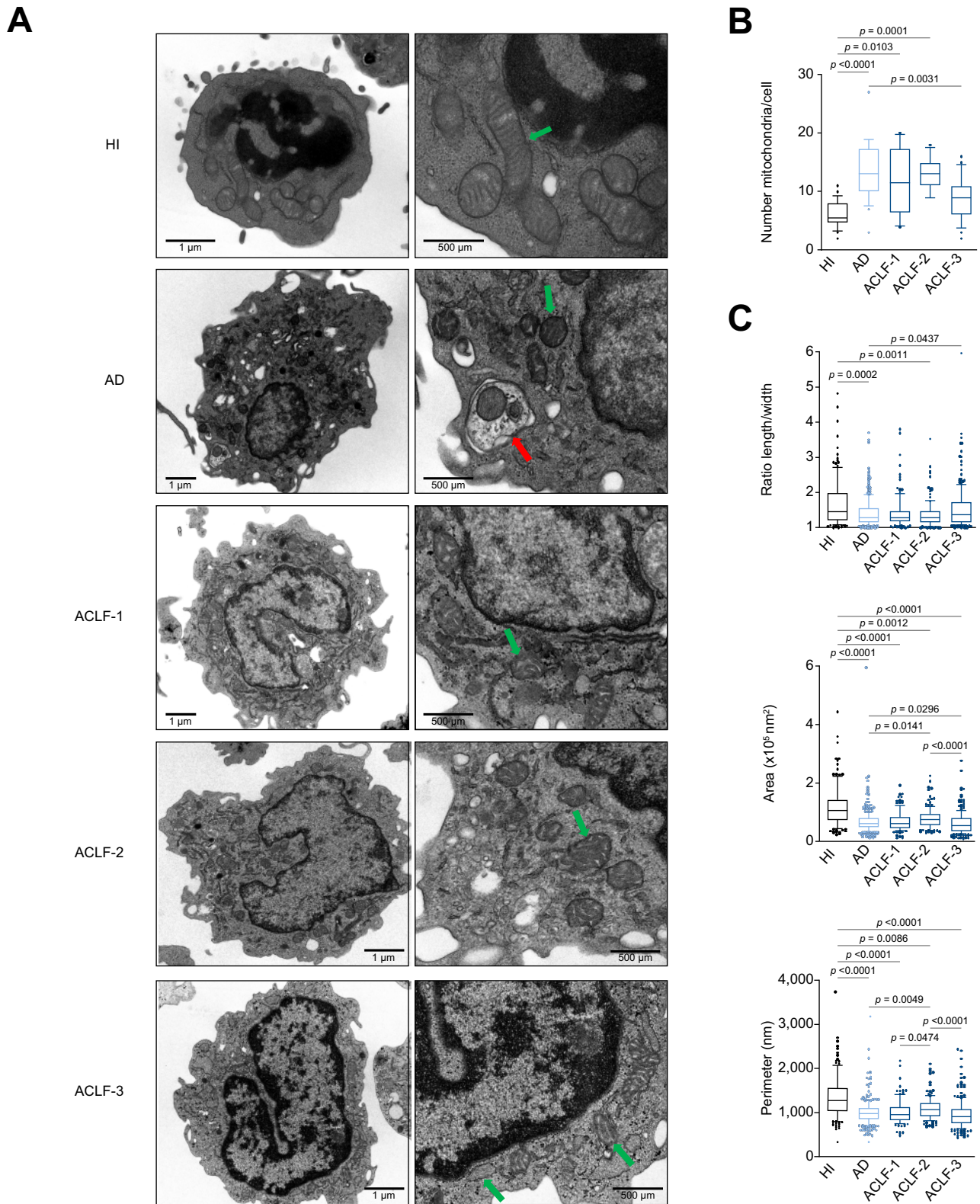


Fig. 1. Patients with AD and ACLF are characterized by altered mitochondrial morphology in leukocytes. (A) Representative electron microscopy images of leukocytes from HIs (n = 3), and patients with AD (n = 3), ACLF-1 (n = 1), ACLF-2 (n = 2) and ACLF-3 (n = 1). Green arrows indicate mitochondria; the red arrow indicates a mitophagic vacuole. (B) Number of mitochondria per cell and (C) length/width ratio, area and perimeter of each mitochondrion. Statistical analysis was performed with Kruskal-Wallis test followed by Dunn's multiple comparisons test. ACLF, acute-on-chronic liver failure; AD, acutely decompensated cirrhosis; HIs, healthy individuals.

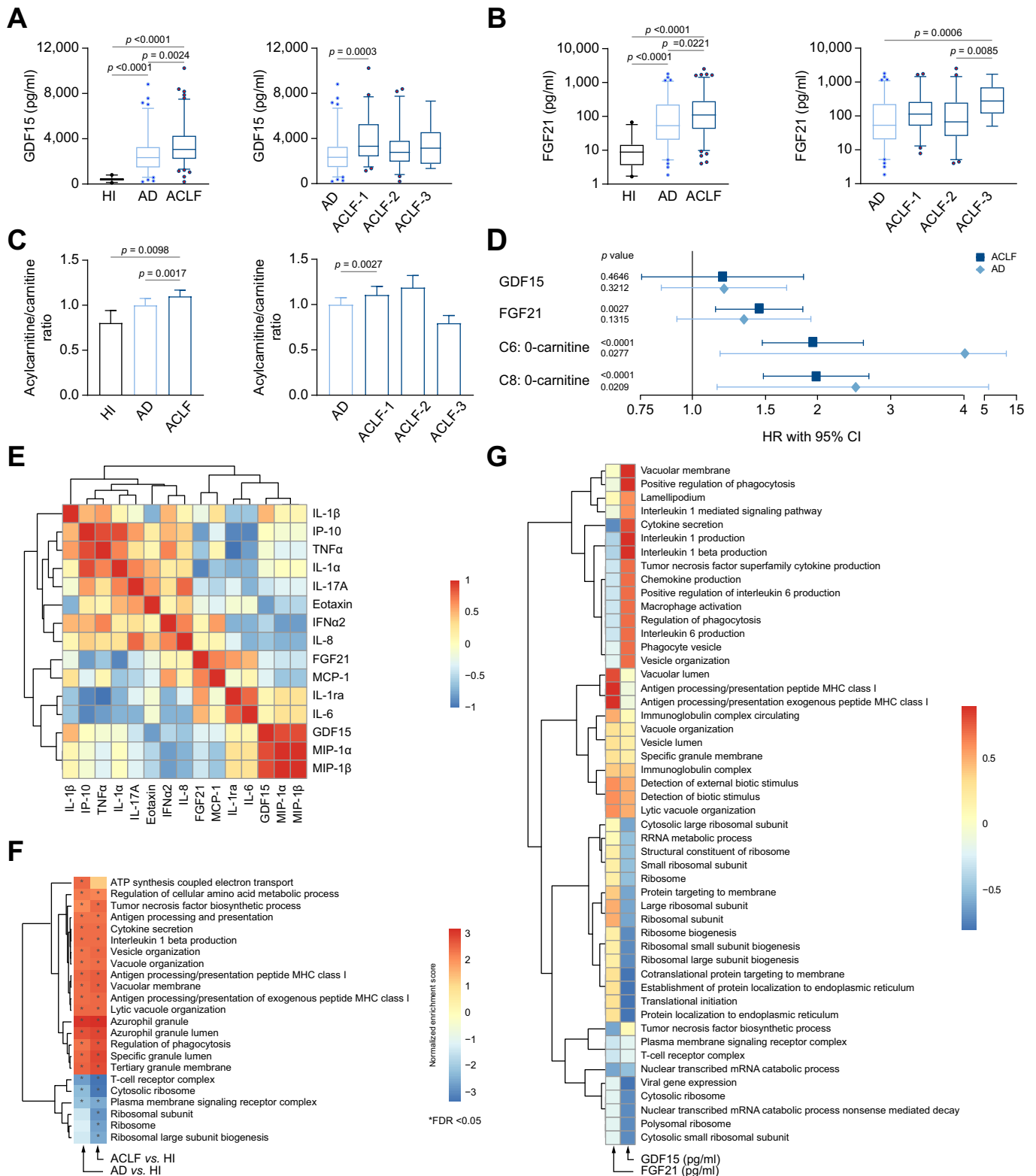


Fig. 2. Plasma biomarkers of mitochondrial dysfunction are elevated in patients with AD and ACLF. (A) Plasma levels of GDF15 in HIs (n = 28), patients with AD (n = 96) and ACLF (n = 115). (B) Plasma levels of FGF21 in the study groups. (C) Blood acylcarnitine/carnitine ratio. Statistical analysis was performed with Kruskal-Wallis test followed by Dunn's multiple comparisons test. (D) Forest plot of multivariate competing risk analysis. Each of the variables were computed in an independent competing risk model with sex and age as covariables. (E) Correlation plot between the mitokines and cytokines/chemokines in patients with ACLF (n = 5). (F) Heatmap of the most significantly differentially regulated gene sets in patients with AD (n = 5) and ACLF (n = 8) vs. HIs (n = 5). (G) Heatmap representing the correlation between GDF15 and FGF21 levels and the normalized enrichment score of the top 50 upregulated gene sets in patients with ACLF (n = 5). ACLF, acute-on-chronic liver failure; AD, acutely decompensated cirrhosis; HIs, healthy individuals.

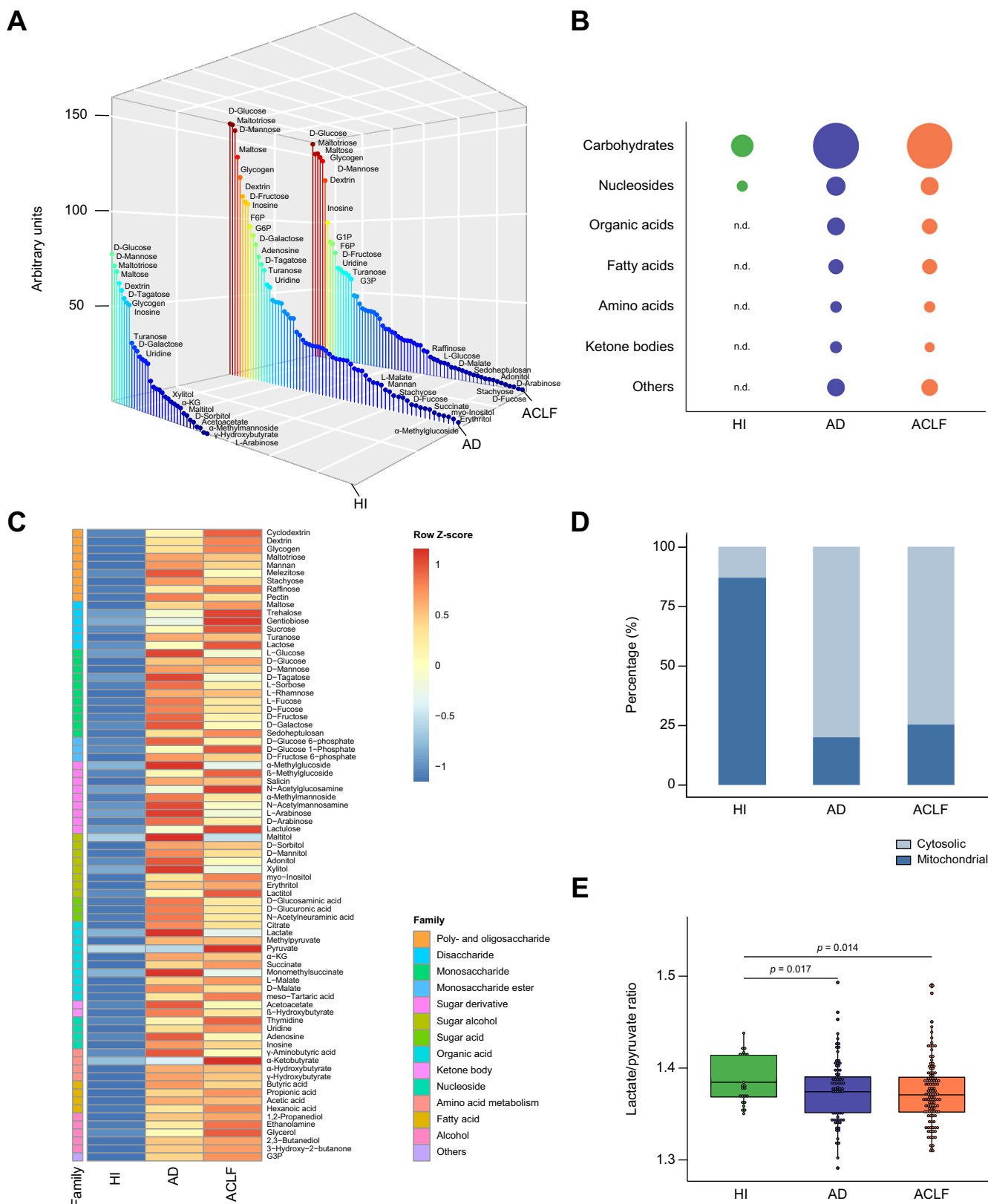


Fig. 3. PBMCs from patients with AD and ACLF utilize a wider set of substrates resulting in considerably higher energy production. (A) 3D bar plots showing substrate/intermediate utilization assessed by whole cell flux analysis in mononuclear leukocytes from HIs (n = 2) and patients with AD/ACLF (n = 4). (B) Bubble chart displaying the utilization of substrates/intermediates shown in A after their assignment to the corresponding macro- and micronutrient family. (C) Supervised clustergram of substrate utilization. Color coding on the left represents the chemical family of each metabolite. (D) Percentage share of the sum of signals of mitochondrial energy production compared to the sum of signals from the whole cell energy output. (E) Plasma lactate/pyruvate ratio in HIs (n = 28), patients with AD (n = 96) and ACLF (n = 115). Statistical analysis was performed with Student's *t* test. ACLF, acute-on-chronic liver failure; AD, acutely decompensated cirrhosis; HIs, healthy individuals; PBMCs, peripheral blood mononuclear cells.

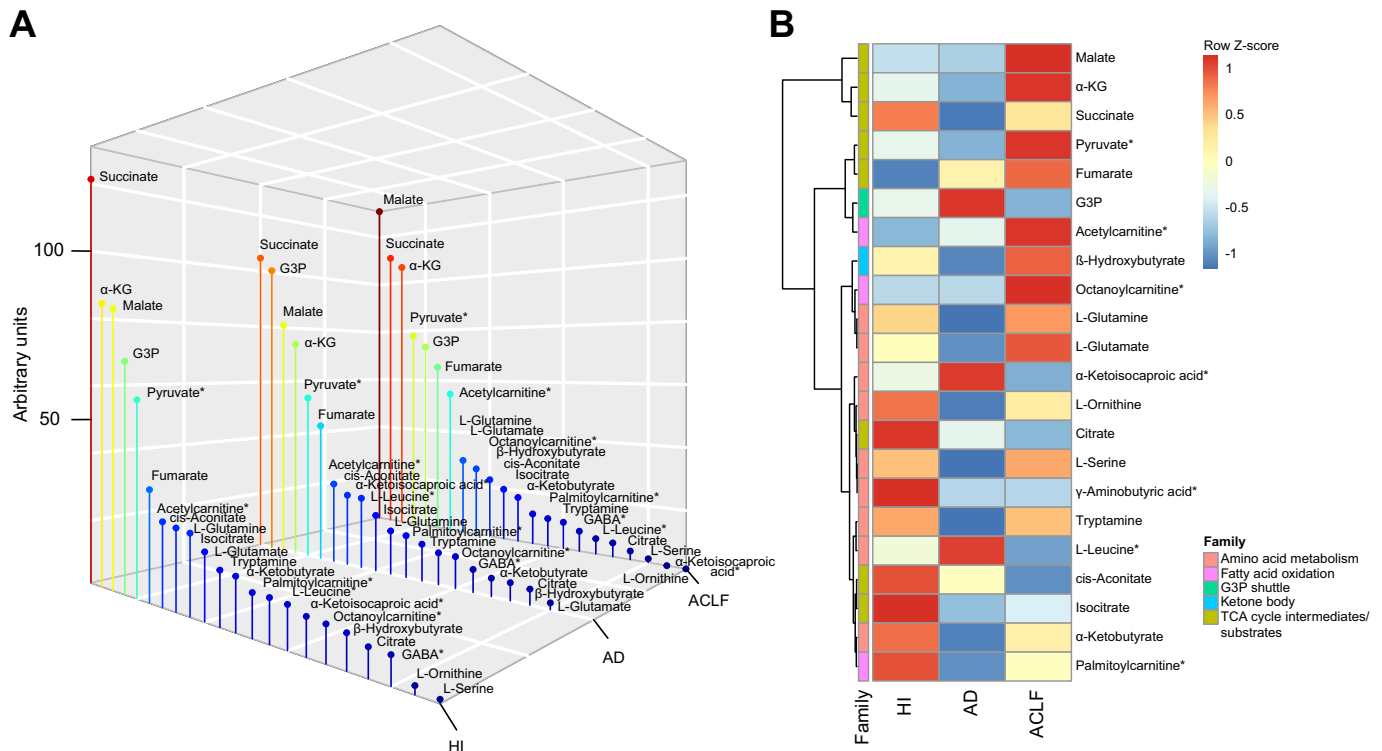


Fig. 4. PBMCs from patients with AD and ACLF do not exhibit a generalized suppression of mitochondrial intermediate utilization. (A) 3D bar plot of substrates/intermediates ranked according to their preferential utilization as determined by mitochondrial function assays in mononuclear leukocytes from HIs (n = 4) and patients with AD/ACLF (n = 5). (B) Unsupervised hierarchical clustergram of the intermediate utilization. Color coding on the left represents the biochemical pathway that each intermediate has been assigned to. *Malate in a concentration of 100 μ M was added to these substrates. ACLF, acute-on-chronic liver failure; AD, acutely decompensated cirrhosis; HIs, healthy individuals; PBMCs, peripheral blood mononuclear cells.

intermediates (*i.e.* malate, α -ketoglutarate [α -KG] and fumarate), acylcarnitines and AAs. The sum of the signals of all substrates/intermediates strictly metabolized in mitochondria revealed that the absolute energy output in AD and ACLF was similar to that of HIs (Fig. S9C). This finding further supports the critical contribution of extra-mitochondrial pathways to the increased energy production needed by PBMCs to satisfy the high energy demand of patients.

Analysis of the TCA cycle reveals two break-points in PBMCs from patients with ACLF

We next ranked the fold regulation obtained by the pairwise comparison of the energy generated from each mitochondrial substrate/intermediate in PBMCs from patients with AD (Fig. 5A) and ACLF (Fig. 5B) with respect to HIs. α -ketoisocaproic acid, L-leucine, G3P, fumarate, L-serine and palmitoylcarnitine were the preferred mitochondrial substrates/intermediates of PBMCs in AD, whereas the rest were less utilized than in HIs (Fig. 5A). In ACLF, acetylcarnitine, C8:0-carnitine, fumarate, L-glutamine, β -hydroxybutyrate and L-glutamate were the 6 most preferred mitochondrial substrates/intermediates, whereas L-ornithine, α -ketoisocaproic acid, citrate, cis-aconitate, L-leucine and isocitrate were the 6 less preferred energy sources (Fig. 5B). Considering only TCA cycle intermediates in the comparison between ACLF and HIs, we were able to identify two break-points: one in the first semicircle of the TCA cycle between isocitrate and α -KG leading to less utilization of upstream intermediates including isocitrate, cis-aconitate and citrate; and the other, in the second semicircle, between succinate and fumarate leading to less

utilization of succinate (Fig. 5C). These two break-points were not observed in patients with AD, in whom only fumarate was more utilized (Fig. 5A), and were less noticeable when comparing ACLF and AD (Fig. S9D). The existence of these two break-points in ACLF suggests that anaplerotic reactions are necessary to replenish the TCA cycle.

PBMCs of patients with AD and ACLF use alternative carbon and nitrogen sources for energy generation

Using volcano plots, we identified that malate, L-glutamine and its derivative L-glutamate were the 3 most relevant metabolites for distinguishing ACLF from AD (Fig. 5D). L-glutamine can be channeled into the TCA cycle via oxidative deamination of L-glutamate to α -KG by glutamate dehydrogenase; α -KG is one of the entry points to the TCA cycle for AA catabolism and also a step in the anaplerotic arginosuccinate shunt.^{22,23} The finding that PBMCs from patients with ACLF engaged more in L-glutamine metabolism was confirmed by testing the energy production from alanyl-glutamine (Ala-Gln), a stabilized delivery form of L-glutamine (Fig. S9E). These data indicate that, in ACLF, PBMCs increasingly used glutaminolysis for anaplerosis of the TCA cycle. In addition, PBMCs from patients with ACLF, and even more so from those with AD, utilized adenosine as an alternative carbon source (Fig. S6-7). Adenosine together with 2,3-butanediol and acetoacetate formed a common signature of substrate utilization by PBMCs in AD and ACLF (Fig. 5E). These data are consistent with recent publications indicating that these patients more actively engage in purine metabolism.⁸

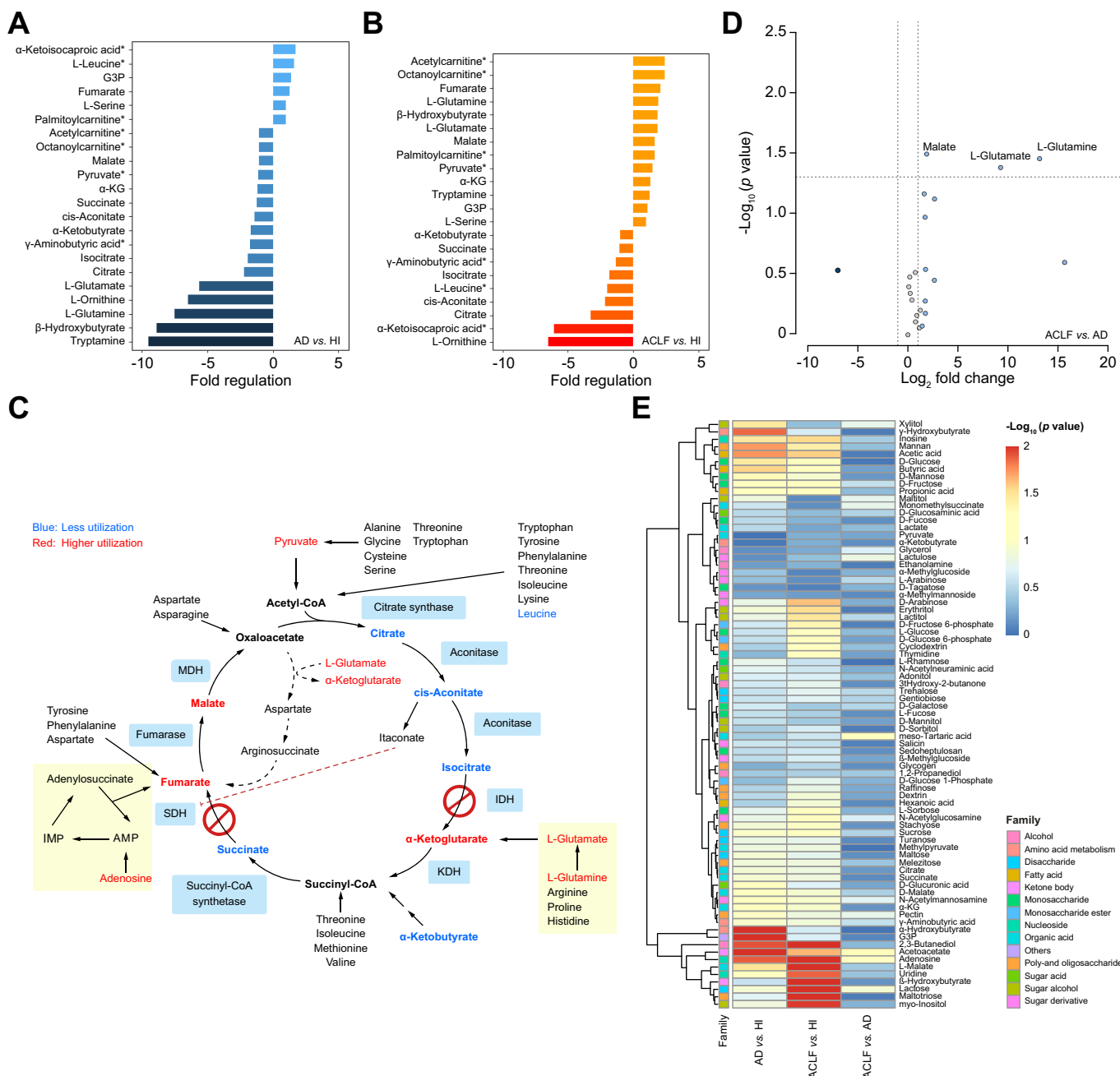


Fig. 5. Analysis by mitochondrial function assays reveals two break-points in the TCA cycle of PBMCs from patients with ACLF. (A) Bar plot of the 22 substrates/intermediates analyzed in the mitochondrial function assay ranked according to their fold regulation between patients with AD and HIs. (B) Ranking of the 22 substrates/intermediates analyzed in the mitochondrial function assay in patients with ACLF compared to HIs. (C) Schematic diagram of the TCA cycle. Metabolites with higher utilization by PBMCs from patients with ACLF compared to those from HIs are indicated in red, and metabolites with less utilization in blue. Anaplerotic pathways are highlighted by yellow shaded background. (D) Volcano plot displaying the results of the pairwise comparison of p values calculated for each metabolite of the whole cell metabolic flux assay. *Malate in a concentration of 100 μ M was added to these substrates. ACLF, acute-on-chronic liver failure; AD, acutely decompensated cirrhosis; HIs, healthy individuals; PBMCs, peripheral blood mononuclear cells; TCA, tricarboxylic acid cycle.

Gene expression analysis of enzymes involved in glucose metabolism

We next performed targeted transcriptomic analysis of genes involved in glucose metabolism in PBMCs from HIs, and patients with AD and ACLF using a Human Glucose Metabolism RT² profiler array. Unsupervised hierarchical cluster analysis identified a cluster (cluster 1) composed of 13 genes encoding cytosolic

enzymes involved in the PPP, glycolysis and glycogen metabolism that were upregulated in PBMCs from patients with AD and ACLF compared to HIs (Fig. 6A). Using volcano plots, we identified that isocitrate dehydrogenase 1 (*IDH1*) was the gene most significantly upregulated in patients with AD compared to HIs (Fig. 6B). *IDH1* produces NADPH which is utilized by cells to counteract oxidative stress.²⁴ Hexokinase 3 (*HK3*), which is the

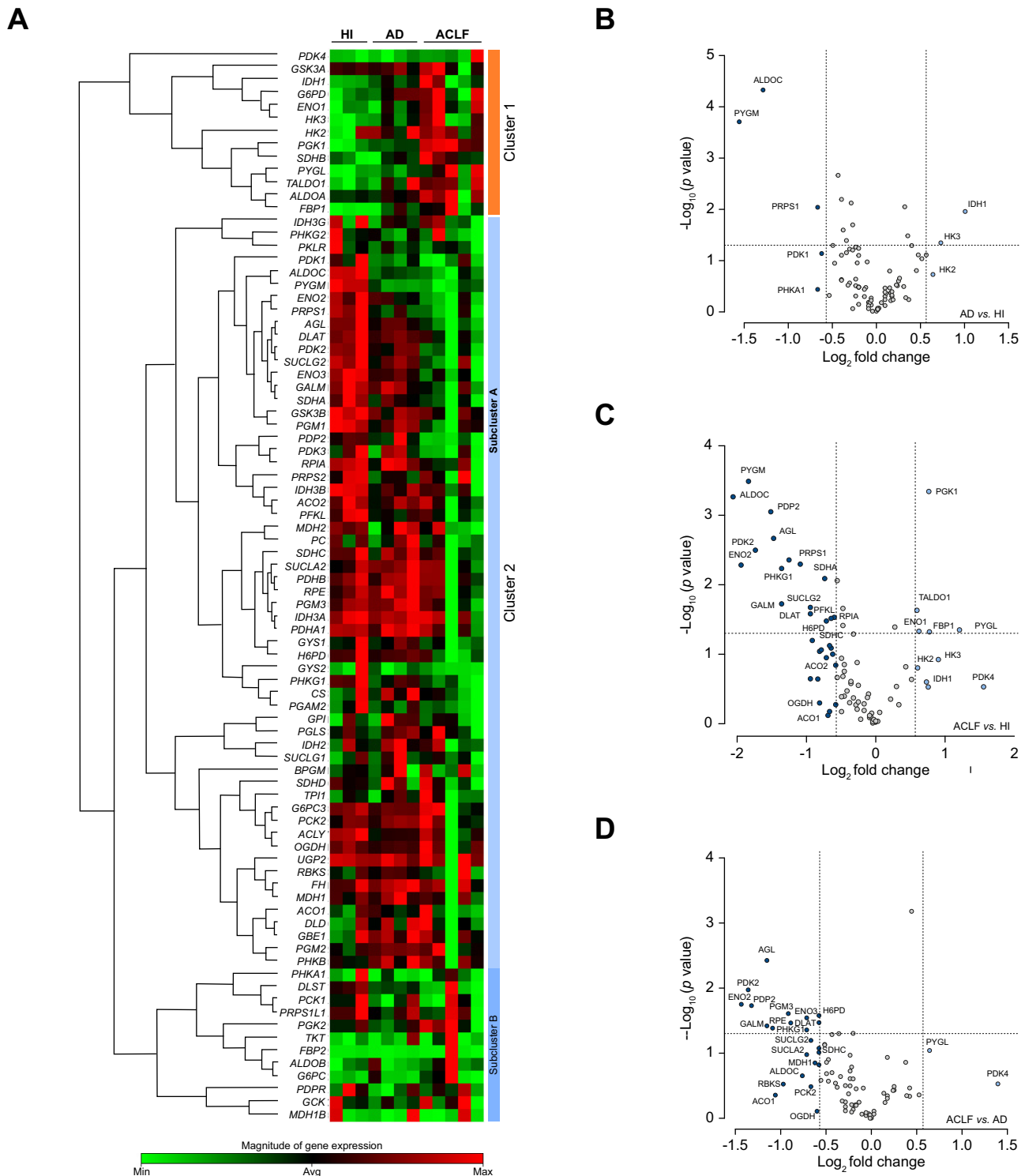


Fig. 6. Expression profile of genes related to glucose metabolism in PBMCs from patients with AD and ACLF. (A) Unsupervised hierarchical clustergram of the PBMC expression of 84 genes related to glucose metabolism. (B-D) Volcano plots comparing AD (n = 4) vs. HIs (n = 3) (B), ACLF (n = 5) vs. HIs (C) and AD vs. ACLF (D). ACLF, acute-on-chronic liver failure; AD, acutely decompensated cirrhosis; HIs, healthy individuals; PBMCs, peripheral blood mononuclear cells.

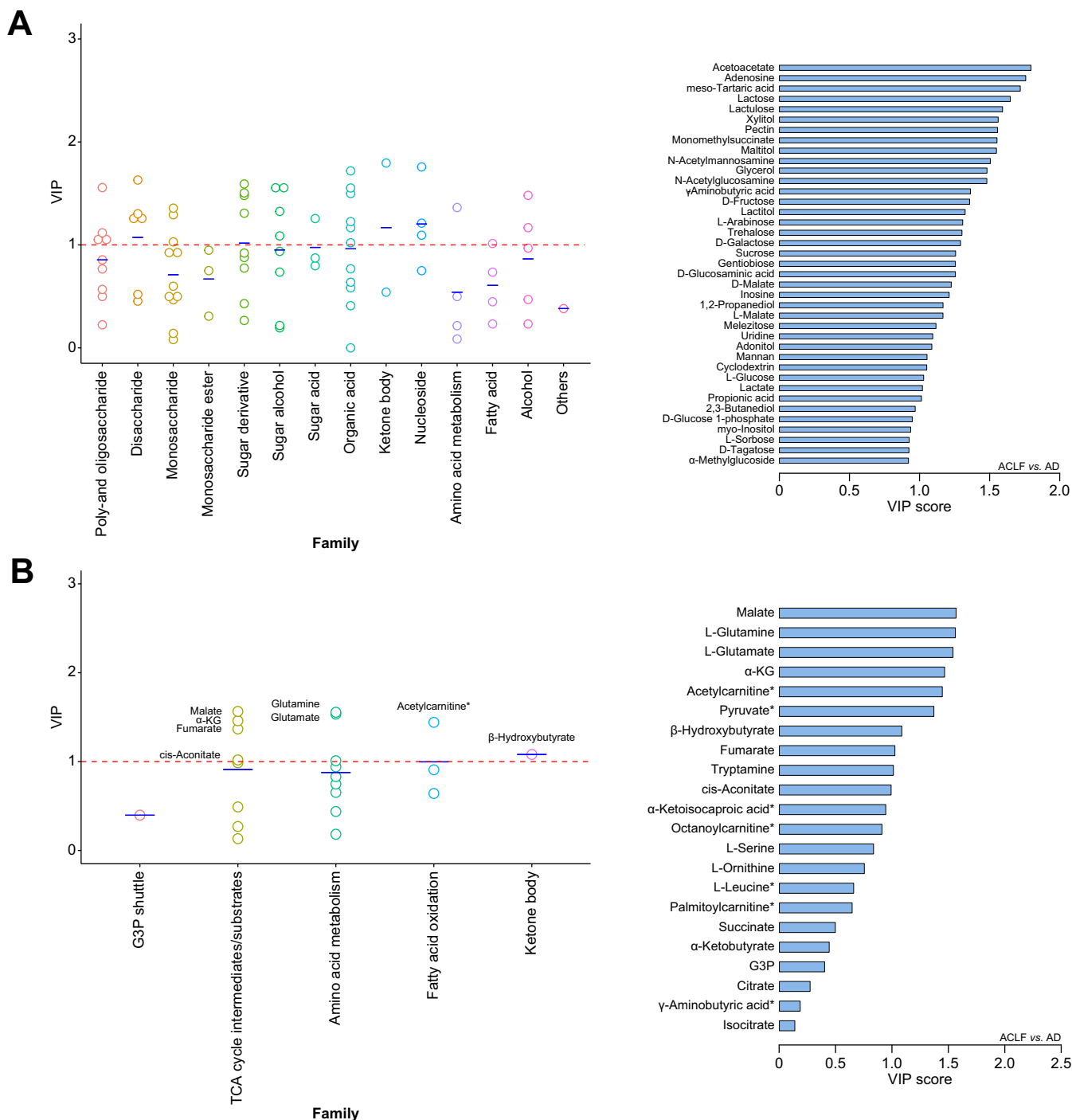


Fig. 7. Identification of metabolites best suited to discriminate metabolism in PBMCs of patients with ACLF. (A) Discriminating accuracy of each chemical family between ACLF and AD (left panel) and metabolites ranked by their VIP score (right panel) as assessed by whole cell flux assays. (B) Discriminating accuracy of each biochemical family between ACLF and AD (left panel) and ranking of each metabolite by its VIP score (right panel), as determined from the mitochondrial function assay. *Malate in a concentration of 100 μ M was added to these substrates. ACLF, acute-on-chronic liver failure; AD, acutely decompensated cirrhosis; PBMCs, peripheral blood mononuclear cells; VIP, variable importance in projection.

most abundant hexokinase in monocytes and catalyzes the first committed step in glycolysis, was the second most significantly upregulated gene in AD compared to HIs (Fig. 6B), underlining the preponderance of glycolysis in AD leukocytes. Comparing patients with ACLF to HIs identified upregulation of genes

involved in glycolysis and PPP (*PGK1*, *ENO1* and *TALDO1*), gluconeogenesis (*FBP1*) and glycogenolysis (*PYGL*) (Fig. 6C). Cluster analysis also identified another cluster (cluster 2) including a subcluster (subcluster A) composed by 59 genes, including *SDHA* (Fig. 6A), that were significantly downregulated

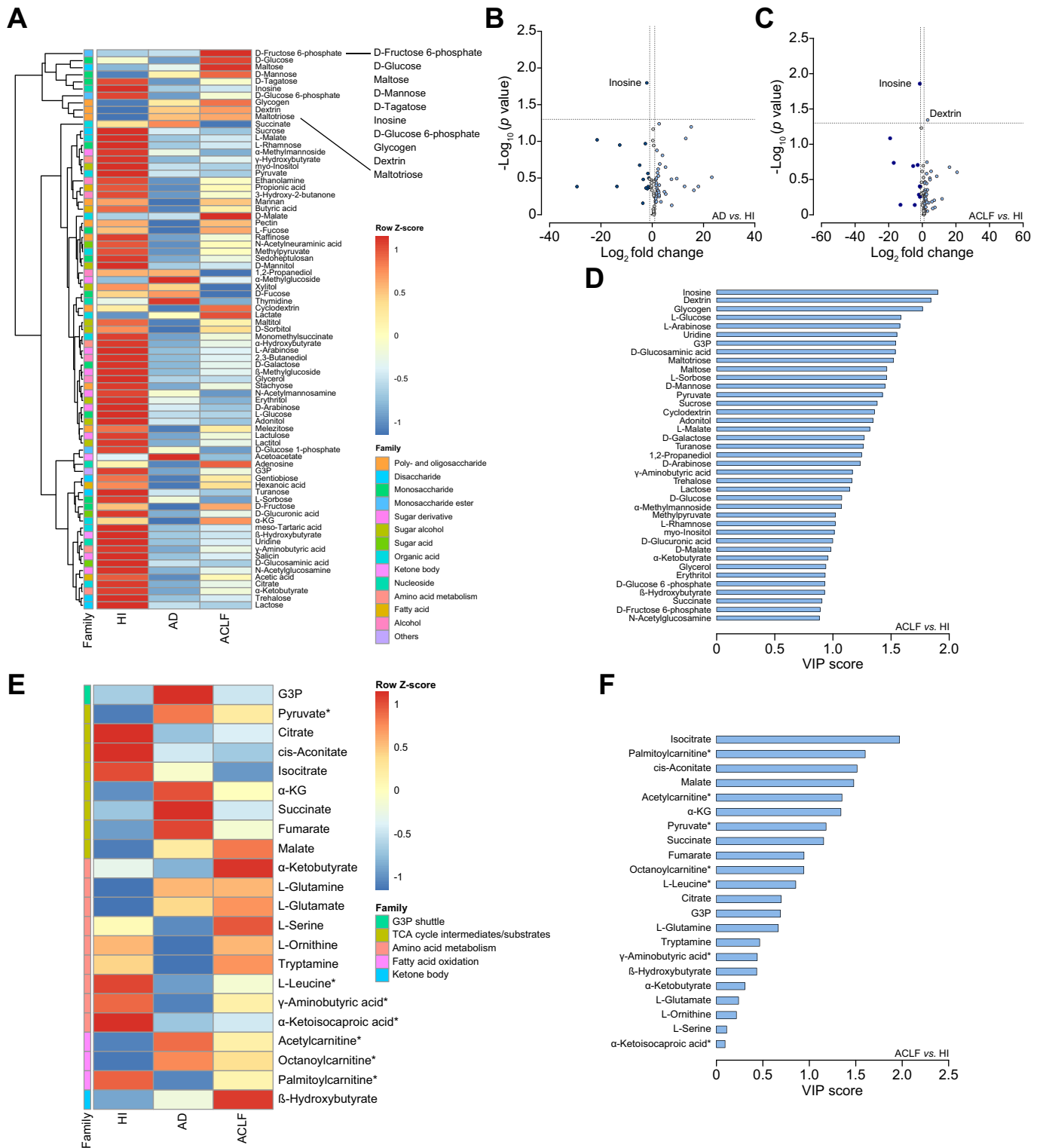


Fig. 8. Analysis of whole cell and mitochondrial fluxes in PMNs from patients with AD and ACLF. (A) Unsupervised hierarchical clustergram of substrate/intermediate utilization in the whole cell flux analysis in neutrophils from HIs (n = 2) and patients with AD/ACLF (n = 4). Color coding on the left represents the chemical family of each metabolite. (B-C) Volcano plot analysis of the whole cell flux analysis comparing AD vs. HIs (B) and ACLF vs. HIs (C). (D) Metabolites discriminating HIs and ACLF as assessed by the whole cell flux analysis, ranked according to their VIP score. (E) Supervised analysis of the substrate/intermediate utilization in mitochondrial function assay in neutrophils from HIs (n = 3) and patients with AD/ACLF (n = 5). Color coding on the left indicates the affiliation of each metabolite to the corresponding biochemical family. (F) Metabolites from the mitochondrial function assay with discriminating power of ACLF, ranked according to their VIP score. *Malate in a concentration of 100 μM was added to these substrates. ACLF, acute-on-chronic liver failure; AD, acutely decompensated cirrhosis; HIs, health individuals; PMN, polymorphonuclear leukocyte; VIP, variable importance in projection.

in ACLF (Fig. 6C). *SDHA* encodes for the major catalytic unit of ETC complex II (succinate dehydrogenase) that oxidizes succinate to fumarate (Fig. S10), and its downregulation is consistent with the break-point in the second TCA semicircle (Fig. 5C). *DLAT* and *PDP2*, which encode for components of the pyruvate dehydrogenase complex (PDC) were also downregulated in ACLF (Fig. 6C). PDC is critical for the decarboxylation of pyruvate into acetyl-CoA, and its downregulation is compatible with the reduction in the lactate/pyruvate ratio observed in these patients (Fig. 3E). The repressed expression of genes involved in pyruvate decarboxylation was also seen in the volcano plot comparing changes between ACLF and AD (Fig. 6D).

Malate and L-glutamine are the best suited mitochondrial metabolites to discriminate ACLF from AD

To reduce the dimension of our dataset and to estimate the discriminatory power of each individual metabolite, we applied partial least square discriminant analysis (PLS-DA) to calculate the variable importance in projection (VIP) scores. We computed the values of whole cell and mitochondrial flux assays separately. In the whole cell flux assay, the best suited metabolites were acetoacetate and adenosine, which attained the highest VIP scores (Fig. 7A). These metabolites were less utilized in ACLF compared to AD (Fig. S8). In the mitochondrial function assay, the best suited metabolites to discriminate ACLF from AD were malate and L-glutamine (and its derivative L-glutamate) (Fig. 7B), which were utilized more in patients with ACLF than in HIs (Fig. 5B) or those with AD (Fig. S9D). Furthermore, they were among the mitochondrial metabolites with the highest fold changes and statistical significance in the volcano plot (Fig. 5D).

Mono- and oligosaccharides are the preferred substrates of PMNs from patients with AD and ACLF

We next performed whole cell flux analysis in PMNs, which are primarily glycolytic cells, with little energy production by mitochondria.²⁵ Indeed, PMNs from HIs showed lower mitochondrial energy production than PBMCs (Fig. S11). Importantly, as opposed to PBMCs, PMNs from the same patients with AD and ACLF produced less energy compared to PMNs from HIs (see the dominant bluish tones in the clustergram in Fig. 8A compared to the reddish tones in Fig. 3C). In addition, PMNs from patients with AD and ACLF used a narrower range of carbon and nitrogen sources to generate energy than those from HIs (Fig. S12A), a finding opposed to that observed in PBMCs (Fig. 3A). Using volcano plots, inosine, the breakdown product of adenosine formed by adenosine deaminase, was identified as the least metabolized substrate by PMNs from patients with AD and ACLF compared to HIs (Fig. 8B,C). Furthermore, inosine was the metabolite with the highest VIP score for ACLF (Fig. 8D). Dextrin was second to this VIP score and its higher utilization in PMNs from patients with ACLF reached statistical significance in the volcano plot (Fig. 8C).

The TCA cycle in PMNs from patients with AD and ACLF is characterized by altered isocitrate catabolism

We next used the mitochondrial function assays and observed that PMNs from AD and ACLF had higher use of intermediates of the second TCA semicircle (i.e. α -KG, fumarate and malate) paralleled by less utilization of intermediates of the first TCA semicircle (i.e. citrate, cis-aconitate and isocitrate) (Fig. 8E,

Fig. S12B). This observation indicates the existence in these cells of one of the two TCA cycle break-points (between isocitrate and α -KG) described above for PBMCs (Fig. 5C). Isocitrate was, in fact, the metabolite that achieved the highest VIP score in patients with ACLF (Fig. 8F).

Discussion

The current investigation characterizes mitochondrial dysfunction at the cellular and organelle level in patients with AD and ACLF. Specifically, we report increased plasma levels of typical biomarkers of primary mitochondrial disorders in these patients. We also provide direct evidence of altered mitochondrial ultrastructure in mononuclear leukocytes, with the most noticeable features being cristae rarefaction and swelling. In addition, we demonstrate the existence of a remarkable metabolic derangement and the association between mitochondrial dysfunction and activation of these immune cells at the transcriptional level. Moreover, we were able to identify a unique signature of mitochondrial alterations specific to ACLF. Altogether, our data leverage the appreciation for the role of mitochondrial dysfunction in advanced cirrhosis to the level of recognition that it has in other critical illnesses, such as sepsis.²⁶ An advantage of our study is that data were obtained in peripheral leukocytes, in which mitochondrial dysfunction is less susceptible to any confounding effect produced by potentially existing hypoxia in tissue.¹¹

Our results confirm that mitochondrial dysfunction is a hallmark of AD and ACLF through the use of easy-to-measure biomarkers. FGF21, which is secreted upon mitochondrial damage,¹⁶ was significantly increased in AD and even more so in ACLF. FGF21 predicted mortality in the latter, a finding that extends those previously described in a Mexican cohort.²⁷ Moreover, our study is the first to show that C6:0- and C8:0-carnitine predict mortality in both AD and ACLF. Therefore, our results encourage the addition of markers of mitochondrial dysfunction to available scoring systems to optimize the prediction of clinical events in patients with ACLF. Notably, GDF15, a useful clinical marker of inborn mitochondrial diseases,¹⁷ strongly correlated with the upregulation of cytokine/chemokine production and the activation of peripheral leukocytes at the transcriptional level, linking mitochondrial damage with immunity. This is an important finding, as leukocytes are the key players in systemic inflammation, which perpetuates tissue injury in advanced cirrhosis.³ However, we could not find a clear correlation between these markers of mitochondrial dysfunction and organ failures. This might be attributed to the fact that distinct cell types with well-described differences in glycolytic activity and capacity for oxidative phosphorylation are represented within a PBMC preparation.²⁸ Studying cell subsets might reveal if certain leukocyte populations are better suited to reflect organ failures. Furthermore, our study was not designed to elucidate whether mitochondrial dysfunction is the underlying cause or the consequence of immune activation, but there is enough evidence supporting that mitochondrial dysfunction at least reinforces and aggravates exaggerated inflammatory responses.²⁹ Mitochondria in turn act as one of the main arbitrators of innate immunity, leading to an overstimulation of the inflammatory system and eventually immune exhaustion.³⁰

Consistent with the well-described high-energy demand of activated immune cells,³¹ mononuclear leukocytes from patients

with AD and ACLF utilize extra-mitochondrial pathways, such as glycolysis, glycogenolysis and PPP, to a much greater extent. In addition, these cells utilized a wider range of carbon and nitrogen sources and a greater diversity of substrates. Another metabolic feature of patients with AD and ACLF is that mononuclear leukocytes exhibit impaired pyruvate decarboxylation to acetyl-CoA. Since this process is mediated by the PDC, which operates at the interface between glycolysis and the TCA cycle, this complex might represent a bottleneck of mitochondrial glucose oxidation in patients with AD and ACLF.

The most relevant finding of our study was that there was not a general “shutdown” of mitochondrial function in mononuclear leukocytes from patients with ACLF but rather selective impairments (break-points) in the TCA cycle. Particularly, by applying mitochondrial function assays, we identified two break-points, one at the isocitrate and the other at the succinate level, resulting in lower turnover of these TCA intermediates in ACLF. This finding is consistent with the elevation of blood citrate/isocitrate and succinate/methylmalonate levels as previously reported.⁷ Similar break-points have been described in M1 macrophages incubated with lipopolysaccharide and interferon- γ as a model of acute inflammation.³² Interestingly, the first isocitrate break-point may lead to the accumulation of upstream TCA intermediates such as cis-aconitate, which is then available for the formation of itaconate, a paradigmatic metabolite connecting cell metabolism with immune responses.³³ In contrast to mononuclear leukocytes, we only found evidence for the first break-point in PMNs from patients with ACLF.

The presence of the above-described break-points in the TCA cycle also revealed the need for anaplerotic pathways to feed the interrupted TCA cycle in mononuclear leukocytes from patients with ACLF. Specifically, we identified increased glutaminolysis and adenosine metabolism as the two most relevant anaplerotic pathways in these patients (Fig. 5C). On one hand, L-glutamine is the most abundant extracellular AA, representing an alternative carbon source to support T cell proliferation, phagocytosis and cytokine production.²³ This 5-carbon backbone AA is utilized at high-rates by immune cells, which are equipped with high mitochondrial glutaminase activity.²³ Favoring glutaminolysis restores the phagocytic and inflammatory capacities of monocytes from patients with ACLF,³⁴ suggesting that it might serve the dual-purpose of energy supply and restoration of phagocytic capacity. On the other hand, adenosine, which was more readily used by mononuclear leukocytes from patients, might be phosphorylated to AMP and enter the cytosolic purine nucleotide cycle (PNC), providing fumarate to bridge the second break-point (Fig. 5C). Indeed, the PNC is recognized as an important player at the cytoplasmic-mitochondrial redox interface in macrophages.³⁵

In summary, our findings provide direct mechanistic evidence of impaired mitochondrial function in peripheral leukocytes from patients with AD and ACLF, underscoring bioenergetic failure as an emerging factor in the pathophysiology of these disease entities. Our study also lays the foundation for the development of useful clinical biomarkers. For instance, based on metabolic flux analysis, we propose that L-glutamine and malate metabolism by mononuclear leukocytes are traits that enable

discrimination between AD and ACLF (Fig. S13). Therefore, future therapeutic strategies aimed at mitochondrial metabolic reprogramming should be encouraged.

Abbreviations

AA, amino acids; ACLF, acute-on-chronic liver failure; AD, acute decompensation; Ala-Gln, alanyl-glutamine; ATF4, activating transcription factor 4; ETC, electron transport chain; FADH₂, reduced flavin adenine dinucleotide; FGF, fibroblast growth factor; GDF, growth differentiation factor; G3P, sn-glycerol 3-phosphate; HIs, healthy individuals; HK, hexokinase; IDH, isocitrate dehydrogenase; α -KG, α -ketoglutarate; PBMC, peripheral blood mononuclear cell; PDC, pyruvate dehydrogenase complex; PLS-DA, partial least squares discriminant analysis; PMN, polymorphonuclear leukocyte; PNC, purine nucleotide cycle; PPP, pentose phosphate pathway; RNA-seq, RNA-sequencing; TCA, tricarboxylic acid; TEM, transmission electron microscopy; VIP, variable importance projection score.

Financial support

Our laboratory is a Consolidated Research Group recognized by the Generalitat de Catalunya (2017SGR1449) and is supported by the Spanish Ministerio de Ciencia e Innovacion (PID2019-105240RB-I00) and EF Clif, a non-profit private organization that receives unrestricted donations from Cellex Foundation, Grifols and European Union's Horizon 2020 research and innovation programme (825694 and 847949). Ingrid W. Zhang is supported by the Sheila Sherlock Post Graduate Programme of the European Association for the Study of the Liver (EASL).

Conflict of interest

The authors declare no conflicts of interest that pertain to this work.

Please refer to the accompanying ICMJE disclosure forms for further details.

Authors' contributions

Study concept and design (IZ, JC); acquisition of samples and data (IZ, MH, DT, JF, CL-V, BC, AMA); contribution to experimental procedures (RF-C, MD-G, MC); bioinformatics and statistical analysis (AC, FA, JLL); data interpretation (IZ, JC); drafting and writing of the final manuscript (IZ, JC); critical revision of the manuscript for important intellectual content (VA); study supervision (JC).

Data availability statement

Gene expression data have been deposited at GEO (accession number GSE180014).

Acknowledgements

We thank María Belén Sánchez, John Cole, Fatima Aziz and Bryan Javier Contreras for their technical assistance and Carles Rentero, Carles Enrich and Glòria Garrabou for helpful comments. We are indebted to the Electron Microscopy Department of the University of Barcelona for technical help.

Supplementary data

Supplementary data to this article can be found online at <https://doi.org/10.1016/j.jhep.2021.08.009>.

References

Author names in bold designate shared co-first authorship

- [1] Moreau R, Jalan R, Gines P, Pavesi M, Angeli P, Cordoba J, et al. Acute-on-chronic liver failure is a distinct syndrome that develops in patients with acute decompensation of cirrhosis. *Gastroenterology* 2013;144:1426–1437. 1437.e1–9.
- [2] Trebicka J, Fernandez J, Papp M, Caraceni P, Laleman W, Gambino C, et al. The PREDICT study uncovers three clinical courses of acutely decompensated cirrhosis that have distinct pathophysiology. *J Hepatol* 2020;73:842–854.
- [3] **Clària J, Stauber RE**, Coenraad MJ, Moreau R, Jalan R, Pavesi M, et al. Systemic inflammation in decompensated cirrhosis: characterization and role in acute-on-chronic liver failure. *Hepatology* 2016;64:1249–1264.
- [4] **Bernsmeier C, van der Merwe S, Périanin A**. Innate immune cells in cirrhosis. *J Hepatol* 2020;73:186–201.
- [5] Mathis D, Shoelson SE. Immunometabolism: an emerging frontier. *Nat Rev Immunol* 2011;11:81–83.
- [6] **Mansouri A, Gattoliat CH**, Asselah T. Mitochondrial dysfunction and signaling in chronic liver diseases. *Gastroenterology* 2018;155:629–647.
- [7] **Moreau R, Clària J**, Aguilar F, Fenaille F, Lozano JJ, Junot C, et al. Blood metabolomics uncovers inflammation-associated mitochondrial dysfunction as a potential mechanism underlying ACLF. *J Hepatol* 2020;72:688–701.
- [8] **Zaccherini G, Aguilar F**, Caraceni P, Clària J, Lozano JJ, Fenaille F, et al. Assessing the role of amino acids in systemic inflammation and organ failure in patients with ACLF. *J Hepatol* 2021;74:1117–1131.
- [9] Garrabou G, Morén C, López S, Tobías E, Cardellach F, Miró Ò, et al. The effects of sepsis on mitochondria. *J Infect Dis* 2012;205:392–400.
- [10] Cheng SC, Scicluna BP, Arts RJW, Gresnigt MS, Lachmandas E, Giamarellos-Bourboulis EJ, et al. Broad defects in the energy metabolism of leukocytes underlie immunoparalysis in sepsis. *Nat Immunol* 2016;17:406–413.
- [11] **Van Wyngene L, Vandewalle J**, Libert C. Reprogramming of basic metabolic pathways in microbial sepsis: therapeutic targets at last? *EMBO Mol Med* 2018;10:1–18.
- [12] **Li P, Wang B**, Sun F, Li Y, Li Q, Lang H, et al. Mitochondrial respiratory dysfunctions of blood mononuclear cells link with cardiac disturbance in patients with early-stage heart failure. *Sci Rep* 2015;5:1–11.
- [13] Koenig MK. Presentation and diagnosis of mitochondrial disorders in children. *Pediatr Neurol* 2008;38:305–313.
- [14] Taylor-Robinson SD, Sargentoni J, Bell JD, Thomas EL, Marcus CD, Changani KK, et al. In vivo and in vitro hepatic phosphorus-31 magnetic resonance spectroscopy and electron microscopy in chronic ductopenic rejection of human liver allografts. *Gut* 1998;42:735–743.
- [15] Phillips MJ. Electron microscopy of the liver. *Postgrad Med* 1967;41:3–14.
- [16] Kim KH, Jeong YT, Oh H, Kim SH, Cho JM, Kim YN, et al. Autophagy deficiency leads to protection from obesity and insulin resistance by inducing Fgf21 as a mitokine. *Nat Med* 2013;19:83–92.
- [17] Montero R, Yubero D, Villarroya J, Henares D, Jou C, Rodríguez MA, et al. GDF-15 is elevated in children with mitochondrial diseases and is induced by mitochondrial dysfunction. *PLoS One* 2016;11:1–15.
- [18] Sharma S, Black SM. Carnitine homeostasis, mitochondrial function and cardiovascular disease. *Drug Discov Today Dis Mech* 2015;6:706–721.
- [19] **Wicks SE, Vandanmagsar B**, Haynie KR, Fuller SE, Warfel JD, Stephens JM, et al. Impaired mitochondrial fat oxidation induces adaptive remodeling of muscle metabolism. *Proc Natl Acad Sci USA* 2015;112:E3300–E3309.
- [20] Hao L, Zhong W, Dong H, Guo W, Sun X, Zhang W, et al. ATF4 activation promotes hepatic mitochondrial dysfunction by repressing NRF1-TFAM signalling in alcoholic steatohepatitis. *Gut* 2020;1–13.
- [21] Williamson DH, Lund P, Krebs HA. The redox state of free nicotinamide-adenine dinucleotide in the cytoplasm and mitochondria of rat liver. *Biochem J* 1967;103:514–527.
- [22] Mills EL, O'Neill LA. Reprogramming mitochondrial metabolism in macrophages as an anti-inflammatory signal. *Eur J Immunol* 2016;46:13–21.
- [23] Newsholme P, Procopio J, Lima MMR, Pithon-Curi TC, Curi R. Glutamine and glutamate—their central role in cell metabolism and function. *Cell Biochem Funct* 2003;21:1–9.
- [24] **Jo SH, Son MK**, Koh HJ, Lee SM, Song IH, Kim YO, et al. Control of mitochondrial redox balance and cellular defense against oxidative damage by mitochondrial NADP⁺-dependent isocitrate dehydrogenase. *J Biol Chem* 2001;276:16168–16176.
- [25] Borregaard N, Herlin T. Energy metabolism of human neutrophils during phagocytosis. *J Clin Invest* 1982;70:550–557.
- [26] **Kraft BD, Chen L**, Suliman HB, Piantadosi CA, Welty-Wolf KE. Peripheral blood mononuclear cells demonstrate mitochondrial damage clearance during sepsis. *Crit Care Med* 2019;47:651–658.
- [27] **Ruiz-Margáin A, Pohlmann A, Ryan P**, Schierwagen R, Chi-Cervera LA, Jansen C, et al. Fibroblast growth factor 21 is an early predictor of acute-on-chronic liver failure in critically ill patients with cirrhosis. *Liver Transpl* 2018;24:595–605.
- [28] **Kramer PA, Ravi S, Chacko B**, Johnson MS, Darley-Usmar VM. A review of the mitochondrial and glycolytic metabolism in human platelets and leukocytes: implications for their use as bioenergetic biomarkers. *Redox Biol* 2014;2:206–210.
- [29] Zhou R, Yazdi AS, Menu P, Tschopp J. A role for mitochondria in NLRP3 inflammasome activation. *Nature* 2011;469:221–226.
- [30] Martin-Mateos R, Alvarez-Mon M, Albillos A. Dysfunctional immune response in acute-on-chronic liver failure: it takes two to tango. *Front Immunol* 2019;10:1–10.
- [31] Kedia-Mehta N, Finlay DK. Competition for nutrients and its role in controlling immune responses. *Nat Commun* 2019;10:1–8.
- [32] Jha AK, Huang SCC, Sergushichev A, Lampropoulou V, Ivanova Y, Loginicheva E, et al. Network integration of parallel metabolic and transcriptional data reveals metabolic modules that regulate macrophage polarization. *Immunity* 2015;42:419–430.
- [33] **O'Neill LAJ, Artyomov MN**. Itaconate: the poster child of metabolic reprogramming in macrophage function. *Nat Rev Immunol* 2019;19:273–281.
- [34] Korf H, Du Plessis J, Van Pelt J, De Groote S, Cassiman D, Verbeke L, et al. Inhibition of glutamine synthetase in monocytes from patients with acute-on-chronic liver failure resuscitates their antibacterial and inflammatory capacity. *Gut* 2019;68:1872–1883.
- [35] Cader MZ, de Almeida Rodrigues RP, West JA, Sewell GW, Md-Ibrahim MN, Reikine S, et al. FAMIN is a multifunctional purine enzyme enabling the purine nucleotide cycle. *Cell* 2020;180:278–295.e23.